JOURNAL OF CHEMICAL INFORMATION AND MODELING

Article

pubs.acs.org/jcim

Molecular Dynamics Approach to Probe the Allosteric Inhibition of PTP1B by Chlorogenic and Cichoric Acid

Sarath Kumar Baskaran, Nabajyoti Goswami, Sudhagar Selvaraj, Velusamy Shanmuganathan Muthusamy, and Baddireddi Subhadra Lakshmi*

Centre for Biotechnology, Anna University, Chennai, India

Supporting Information

ABSTRACT: Protein tyrosine phosphatase 1B (PTP1B), a major negative regulator of the insulin and leptin signaling pathway, is a potential target for therapeutic intervention against diabetes and obesity. The recent discovery of an allosteric site in PTP1B has created an alternate strategy in the development of PTP1B targeted therapy. The current study investigates the molecular interactions between the allosteric site of PTP1B with two caffeoyl derivatives, chlorogenic acid (CGA) and cichoric acid (CHA), using computational strategies. Molecular docking analysis with CGA and CHA at the allosteric site of PTP1B were performed and the resulting protein−ligand complexes used for molecular dynamics simulation studies for a time scale of 10 ns. Results show stable binding of CGA and CHA at the allosteric site of PTP1B. The flexibility of the WPD loop was observed to be constrained by CGA and CHA in the open (inactive), providing molecular mechanism of allosteric inhibition. The allosteric inhibition of CGA and CHA of PTP1B was shown to be favorable due to no restriction by the α-7 helix in the binding of CGA and CHA at the allosteric binding site. In conclusion, our results exhibit an inhibitory pattern of CGA and CHA against PTP1B through potent binding at the allosteric site.

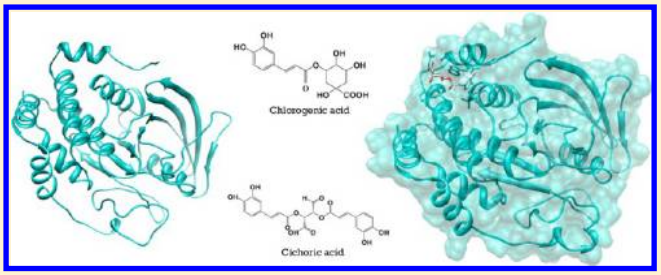

INTRODUCTION

Protein tyrosine phosphatases (PTPases) belong to a diverse family of enzymes that cause selective dephosphorylation of tyrosine residues in the various signal transduction pathways.[1,23,4] The PTPases are mainly characterized by their signature motif known as the PTP loop consisting of HCXAGXGR that includes the active site Cys 215.[5] Among the various PTPases, PTP1B acts as a major negative regulator of both insulin and leptin signaling, a dysfunction of which is commonly associated in disease states such as diabetes and obesity.[6,7] Reports have indicated that PTP1B knockout mice resulted in an increased insulin sensitivity as measured by improved glucose clearance.[8,9] PTP1B, a cytosolic soluble monomeric enzyme (50 kDa), has been observed to play a crucial role in the dephosphorylation of the insulin receptor, thereby showing promise as an effective drug target in the treatment of type II diabetes and obesity,[10−12] leading to an increased interest toward identification of potent PTP1B inhibitors.[13] Structurally, the canonical form of PTP1B is made up of 435 amino acids constituting the soluble form whereas the shorter 282, 298, or 321 residue length fragment is typically used in most biochemical and biological studies (see Figure 1).[14,15] The active site of PTP1B consists of His 214−Arg 221 (PTP loop) also known as the P loop. Just above the active site, closing over the binding pocket is the WPD loop (Trp 179, Pro 180, Asp 181) encompassing residues from Thr 177 to Pro 185.[15,16] Along with these residues, a few other amino acids such as Lys 120, Gln 262, Val 49, Arg 47, Phe 182, and Tyr 46

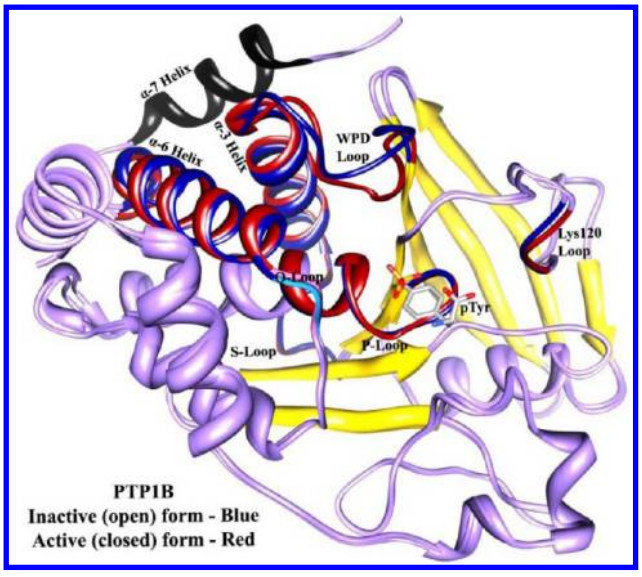

Figure 1. Structure of PTP1B labeled with the significant regions (1T49 superimposed with 1SUG). The substrate pTyr is represented as a stick model (colored by atom type), the WPD (open, inactive state) is shown in blue with α-3 and α-6 helices, and the WPD (closed, active state) is shown in red with α-3 and α-6 helices at the active state. The α-7 helix is shown in black.

Received: December 7, 2011

   dx.doi.org/10.1021/ci200581g | J. Chem. Inf. Model. XXXX, XXX, XXX−XXX

considerably contribute to peptide substrate recognition by a combination of electrostatic, hydrophobic, and hydrogen-bonding interactions.[17]

In the Apo (inactive) form, the WPD loop is usually in an "open" conformation (WPD open), whereas it twists over the active site Cys 215 upon binding of the pTyr substrate causing the "closed" conformation (WPD closed) of the catalytic loop resulting in the activation of the protein.[18] The role of the WPD loop in PTP1B, particularly a conformational change after substrate binding, has been well studied and established that closure of the WPD loop is an essential event in the catalytic mechanism of PTP1B.[19]

The current status of all the recent and efficient PTP1B inhibitors has been clearly reviewed by Doina Popov.[20] The most common strategy is to incorporate nonhydrolyzable phosphotyrosine analogs or other structural scaffolds by targeting the active catalytic site.[21−33] Although many potent inhibitors have been developed, they predominantly fail to progress beyond the preclinical stage.[34,35] Compounds that bind effectively to the PTP1B active site tend to be charged, thereby limiting their permeability to the cell-membrane, in addition to requiring modifications such as esterification to improve intracellular delivery.[36] Studies on TC-PTP (T-cell Protein tyrosine phosphatase) the most homologous phosphatase to PTP1B with 74% sequence identity in the catalytic domain have shown that TC-PTP null mice die within 5 weeks of age, and the TCPTP gene to be associated with human inflammatory diseases.[37]

Interestingly, Wiesmann et. al[38] described a group of non-pTyr-like allosteric inhibitors (compound-2) binding to a novel site located ∼20 Å away from the catalytic site. This allosteric site flanked by α-3, α-6, and α-7 helices was observed to be a promising alternate regulatory site triggering PTP1B inhibition by altering the interaction of the α-3 and α-6 helix with the α-7 helix. The allosteric inhibitor (compound-2) was perceived to bind between α-3, α-6, and α-7 and observed to stabilize the WPD loop in the Apo conformation, thus constraining the activation of PTP1B. Targeted molecular dynamics simulation studies on PTP1B have reported the movement of the catalytic WPD loop closure and postulated that the reduced mobility of WPD loop is accompanied by reduced mobility of the S-loop in addition to H-bond interaction between Trp 179 and Arg 221.[39−41]

Therefore, allosteric modulation of PTP1B activity with small molecules might provide a promising approach to overcome the potential challenges of targeting the active site. Earlier in vitro and in vivo experiments from our lab have clearly shown the role of chlorogenic acid and other caffeoyl derivatives isolated from *Cichorium intybus* in insulin signaling through PTP1B inhibition.[42,43] Hence, evaluation of these compounds as allosteric inhibitors using an integrated docking and molecular dynamics approach has been attempted.

MATERIALS AND METHODS

PTP1B Inhibition Assay. PTP1B inhibition assay was performed as described previously with minor modifications.[38,43] Briefly, 25 ng of recombinant PTP1B enzyme (Cayman chemicals, USA) was incubated with logarithmic concentrations of chlorogenic acid (CGA) and cichoric acid (CHA) for 10 min in assay buffer at 37 °C. The reaction was initiated by the addition of 20 mM pNPP (Merck, India), incubated at 37 °C for 30 min, and the activity of the enzyme was measured at 405 nm against reagent blank (Multiscan Plate Reader, Thermo, USA). Sodium orthovanadate was used as positive control. For competitive binding assay, IC_{50} concentrations of CGA and CHA (10 μM) were coincubated with logarithmic dose of SOV and activity measured as above.

Molecular Docking. Molecular docking has been used a tool for the computational design and discovery of novel PTP1B inhibitors[44−47] and there have been reports on the evaluation of the binding efficacy of protein targets using AUTODOCK.[48−52] The coordinates of the ligand molecules, chlorogenic acid (1*S*,3*R*,4*R*,5*R*)-3-{[(2*Z*)-3-(3,4-dihydroxyphenyl)prop-2-enoyl]oxy}-1,4,5-trihydroxycyclohexanecarboxylic acid and cichoric acid (2*R*,3*R*)-2,3-bis{[(E)-3-(3,4-dihydroxyphenyl)prop-2-enoyl]oxy}butanedioic acid were obtained in PDB format from the PRODRG server[53] and energy minimized for 1000 steps using UCSF Chimera.[54] The crystal structure of PTP1B from 1T49 (open, inactive) with compound-2 (IUPAC name: 3-(3,5-dibromo-4-hydroxybenzoyl)-2-ethyl-benzofuran-6-sulfonic acid (4-sulfamoylphenyl)-amide) as the allosteric inhibitor and PTP1B from 1SUG (closed, active) were used in the study. The receptor protein structure of PTP1B in native (open, inactive) conformation was selected from PDBID 1T49 (with truncated α-7 helix) and optimized for rigid docking (flexible ligand to rigid protein) using the Autodock Tools—ADT 1.5.6.[55] Molecular docking of the two caffeoyl derivatives with the PTP1B structure were performed individually using AUTODOCK v 4.2[56] with maximum number of active torsions allowed for each ligand. The docking analysis was performed in a grid box of 52 × 52 × 52 with a grid spacing of 0.375 Å centered on the position of the allosteric site (enclosed between α-3, α-6, and α-7 helices) of PTP1B. The 20 best conformations were selected from a population of 150 individuals based on their empirical free energy of binding and calculated using the Lamarckian genetic algorithm.[57] The parameters for docking were optimized by repeated docking of compound-2 (ligand in 1T49) with PTP1B to possibly get the best conformation of compound-2 with the reported interactions (Supporting Information Figure 1). The best conformation with least binding energy and better interacting residues was selected. The hydrogen bond predictions were considered within a maximum distance of 3.0 Å.

Modeling of α-7 Helix to the Protein. The α-7 helix enclosing the allosteric site of PTP1B was found to play a significant role in the inactivation of the protein.[38,41] Since, experimental PTP1B structure in the open form of the WPD loop along with the α-7 helix is not available in the PDB, we have modeled the α-7 helix to 1T49 and investigated the role of the α-7 helix in the allosteric inhibition of PTP1B. The modeling of the α-7 helix to PTP1B (native, open form) was performed by homology modeling with 1SUG (active, closed form) using MODELER 9v7.[58] This modeling of the α-7 helix was done on PTP1B, 1T49, the PTP1B−chlorogenic acid complex, and the PTP1B−cichoric acid complex.

Molecular Dynamics Simulations. Various reports on the atomistic interaction of PTP1B with and without ligands have enumerated the facts behind the flexibility and effectiveness of the PTP1B inhibitors using molecular dynamics simulation.[39−41,59−62] We have performed the molecular dynamics calculations with and without the modeled α-7 helix to probe the role and flexibility of the helix in the inhibition of PTP1B

dx.doi.org/10.1021/ci200581g | J. Chem. Inf. Model. XXXX, XXX, XXX−XXX

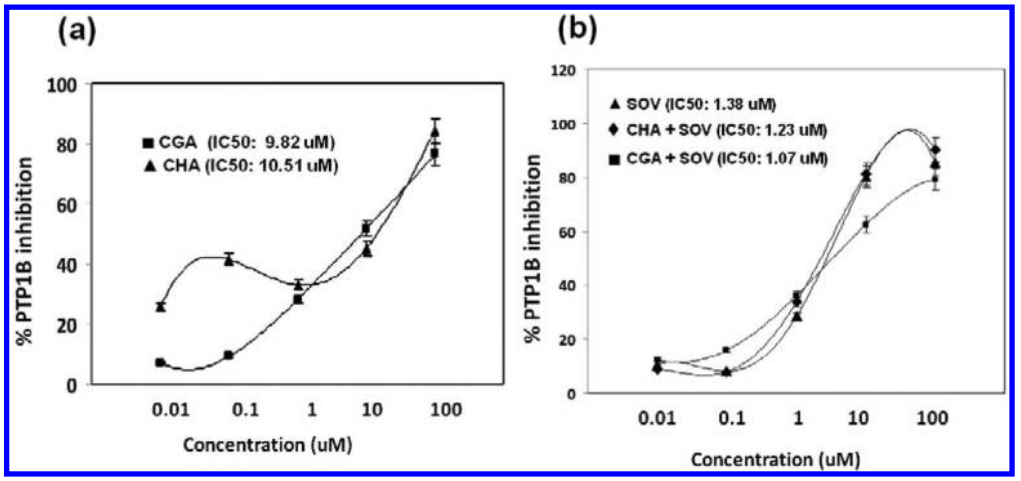

Figure 2. (a) Inhibitory effect of CGA and CHA against PTP1B enzyme. CGA and CHA activity is expressed as percent PTP1B inhibition, and IC_{50} was determined as 10 μM for both. (b) IC_{50} concentrations of CGA and CHA (10 μM) was coincubated with a logarithmic dose of SOV, and the inhibitory pattern is shown as percent PTP1B inhibition.

for a time scale of 10 ns. Eight simulations were performed and are represented as follows:

(a) $PTP1B_{1\text{-}298a}$ native PTP1B without inhibitor with modeled α-7 helix
(b) $PTP1B_{1\text{-}298b}$ PTP1B with compound-2 with modeled α-7 helix
(c) $PTP1B_{1\text{-}298c}$ PTP1B with chlorogenic acid with modeled α-7 helix
(d) $PTP1B_{1\text{-}298d}$ PTP1B with cichoric acid with modeled α-7 helix
(e) $PTP1B_{1\text{-}282e}$ native PTP1B without inhibitor without α-7 helix
(f) $PTP1B_{1\text{-}282f}$ PTP1B with compound-2 without α-7 helix
(g) $PTP1B_{1\text{-}282g}$ PTP1B with chlorogenic acid without α-7 helix
(h) $PTP1B_{1\text{-}282h}$ PTP1B with cichoric acid without α-7 helix

The simulations were performed for a time scale of 10 ns each, with a united-atom force field using the GROMACS 4.0.5 package.[63,64] Since compound-2 is the only known allosteric inhibitor of PTP1B until now, compound-2 (from 1T49) was taken as the reference ligand. Simulations were performed for compound-2 (docking predicted) with PTP1B in the presence and absence α-7 of helix for validation (data not shown). The topology files necessary for the simulation were calculated and obtained using PRODRG.[53] Initially, protonation states were added to the protein residues at a pH-7, and the protein−ligand complex was simulated with explicit water model in a water box of 1.2 nm from the surface of the protein. The system was neutralized with counterions and energy minimization was performed using steepest descent for 3000 steps. The protein backbone was then frozen, and solvent molecules with counterions were allowed to move during a 50 ps position restrained molecular dynamics (MD) run. Finally 10 ns of production MD run were performed. The electrostatic interactions were calculated by the Particle Mesh Ewald (PME) algorithm, with an interpolation order of 4 and a grid spacing of 0.12 nm. All simulations were run under periodic boundary conditions with an *NPT* ensemble using Berendsen's coupling algorithm for keeping the temperature (300 K) and the pressure (1 bar) constant. The SHAKE algorithm with a tolerance of 10^{-5} Å was applied to fix all bonds containing hydrogen atoms. The time step for the simulations was 2 fs, and the coordinates were stored every 2 ps. The van der Waals (vdw) forces were treated using a cutoff of 12 Å. The analysis of trajectories was performed using GROMACS 4.0 package,[63,64] and the plots were viewed using GRACE.[65]

RESULTS AND DISCUSSION

PTP1B Inhibition. To demonstrate the inhibitory effect of CGA and CHA, recombinant human PTP1B enzyme was incubated with logarithmic concentrations of CGA and CHA, resulting in a dose dependent inhibition of PTP1B activity with an IC_{50} value of 10 μM (Figure 2a). Further, the IC_{50} concentrations of CGA and CHA were tested along with logarithmic doses of sodium orthovanadate (SOV), a known competitive catalytic site inhibitor of PTP1B, to understand the inhibitory pattern of CGA and CHA. Our result shows that the coincubation of CGA and CHA with SOV does not affect the inhibitory pattern of SOV (Figure 2b). Since noncompetitive inhibitors can simultaneously bind to PTP1B along with SOV (competitive inhibitor) and do not interfere with the SOV inhibitory pattern, we postulate that both CGA and CHA inhibit PTP1B activity in a noncompetitive manner. Hence, we analyzed the molecular level interaction between the compounds and PTP1B.

Molecular Docking of CGA and CHA at the Allosteric Site of PTP1B. Molecular docking analysis was performed to study the binding energy and probe the interaction between the PTP1B allosteric site with the compounds (CGA and CHA; Figure 3). The best conformation with least binding energy and most number of H-bonds between the compounds and PTP1B was selected from a group of 20 possible conformations scrutinized from a population of 150 individuals for the study. Docking analysis of PTP1B (1T49 with the ligand removed) and compound-2 was performed to validate the procedure (data not shown).

Both CGA and CHA exhibit better interaction with the allosteric site of PTP1B in comparison to compound-2. Figure 4a shows the best conformation of CGA and PTP1B with the least binding energy of −5.85 kcal/mol, forming H-bond interactions with Asn 193, Ala 189, Glu 200, and two H bonds with Lys 197, and Figure 4b shows the best conformation of

dx.doi.org/10.1021/ci200581g | J. Chem. Inf. Model. XXXX, XXX, XXX−XXX

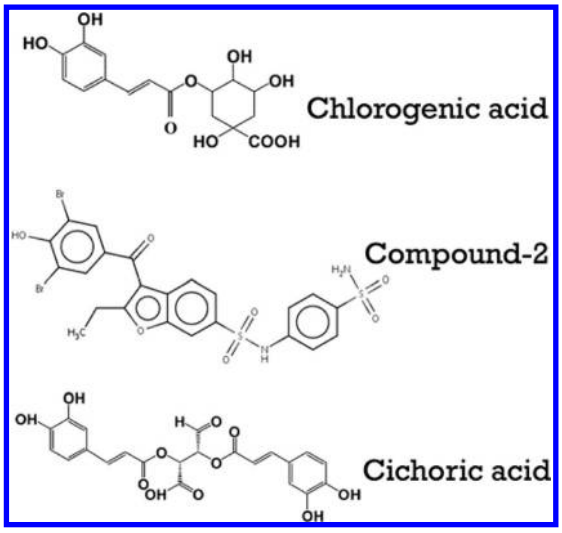

Figure 3. Structure of chlorogenic acid (CGA), compound-2, and cichoric acid (CHA).

CHA with PTP1B with the least binding energy of −5.74 kcal/mol forming H-bond interactions with Asn 193, two H-bond interactions with Glu 276, and two H-bond interactions with Ile 281. These conformations were taken for molecular simulations.

Molecular Dynamics Analysis of CGA and CHA with the Allosteric Site of PTP1B. Molecular dynamics analysis was performed to investigate the molecular interaction efficacy of CGA and CHA with allosteric site of PTP1B. To study the role of the α-7 helix in the allosteric inhibition of PTP1B, the α-7 helix was modeled to the PTP1B (1T49) and simulation carried out with the modeled α-7 helix in the absence of ligand and considered as free native protein with the open active state of the WPD loop ($PTP1B_{1\text{-}298a}$). The $PTP1B_{1\text{-}298a}$ with the reference ligand compound-2 was considered as reference ligand−protein complex ($PTP1B_{1\text{-}298b}$). The simulation of CGA ($PTP1B_{1\text{-}298c}$) and CHA ($PTP1B_{1\text{-}298d}$) with $PTP1B_{1\text{-}298a}$ was performed and compared with reference ligand−protein simulation $PTP1B_{1\text{-}298b}$.

Preliminary analysis of the root mean square deviation shows that $PTP1B_{1\text{-}298a}$ starts to stabilize from 2 ns and was sufficiently maintained with minimal deviations after 4 ns for the entire

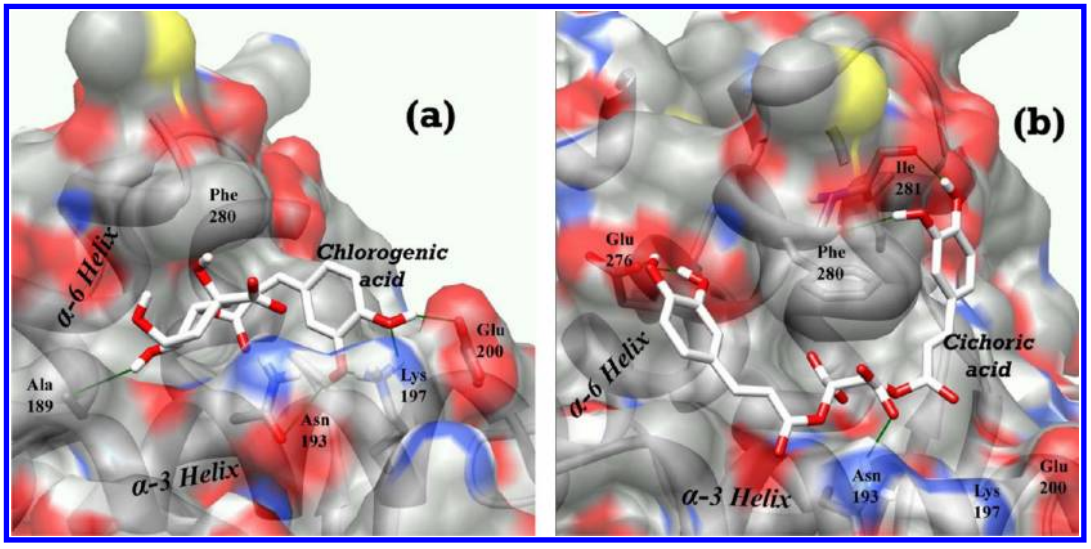

Figure 4. Best conformations of CGA (a) and CHA (b) shown as thick stick models with the allosteric site of PTP1B with α-3 and α-6 helices (ribbon model shown with transparent molecular surface colored by atom type). The residues forming interactive H-bonds with the compounds are labeled black.

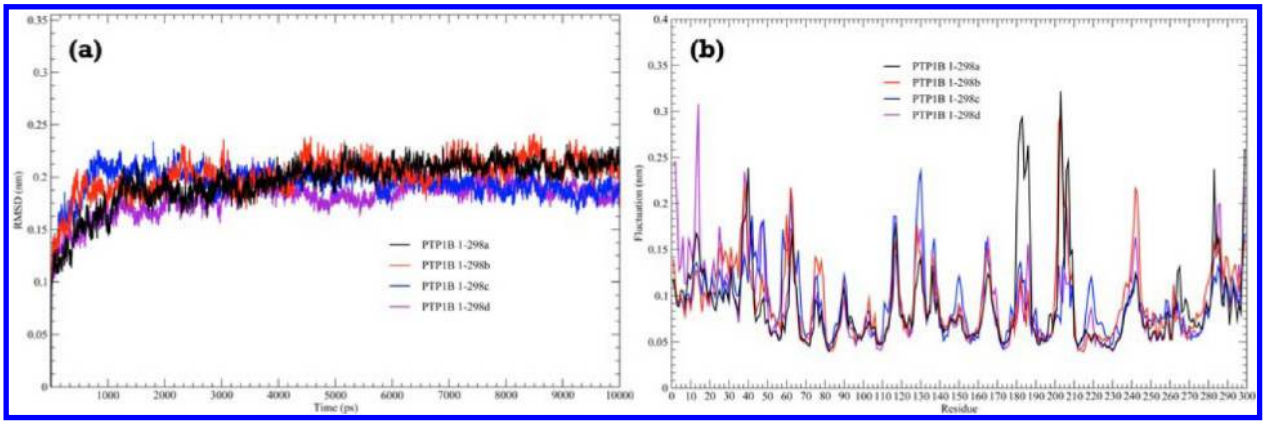

Figure 5. (a) Root mean square deviation profile of PTP1B (protein after least-squares fit to backbone) in the presence and absence of inhibitors depicted for the entire 10 ns simulation in the presence of α-7 helix. (b) Root mean square fluctuation (α-carbon of each residue) in the presence and absence of inhibitors comparatively depicted for the entire 10 ns simulation in the presence of α-7 helix.

dx.doi.org/10.1021/ci200581g | J. Chem. Inf. Model. XXXX, XXX, XXX−XXX

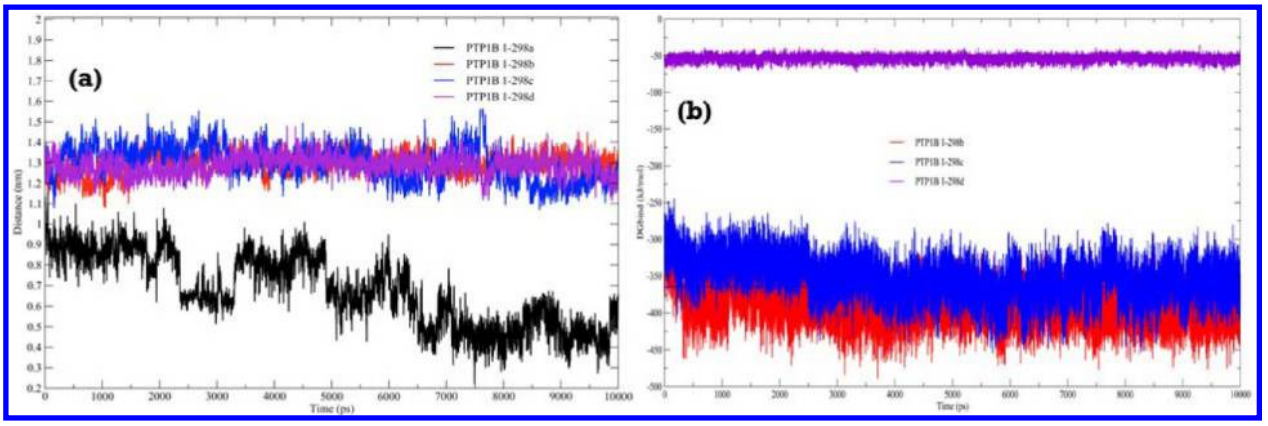

Figure 6. (a) Distance deviation profile of Asp 181 of the WPD loop with Cys 215 of the P loop at the catalytic site in the presence and absence of inhibitors depicted for the entire 10 ns simulation. (b) Linear interaction binding free energy estimate of PTP1B with the inhibitors for the entire 10 ns simulation.

period of simulation (Figure 5a). The protein−ligand complexes $PTP1B_{1\text{-}298b}$, $PTP1B_{1\text{-}298c}$, and $PTP1B_{1\text{-}298d}$ were observed to be stabilized from 4 ns with very small deviations being observed during the course of stabilization

Comparative analysis of the RMSF profile of the native protein and protein with the bound allosteric inhibitors (Figure 5b) indicates a fluctuation of 3.0 Å at the WPD loop (177−185) for native protein $PTP1B_{1\text{-}298a}$, whereas no significant fluctuation was observed with $PTP1B_{1\text{-}298b}$, $PTP1B_{1\text{-}298c}$, and $PTP1B_{1\text{-}298d}$ and reduced fluctuation at the WPD region was observed in $PTP1B_{1\text{-}282e}$ (Supporting Information Figure 2). Although few of the regions of the protein exhibit high mobility, they are not considered significant for the study since the major dynamic change with the ligand was observed at the catalytic WPD loop.

An important functional structural region of PTP1B, the WPD loop determines the activity of the protein by moving Asp 181 over the Cys 215 at the catalytic site and closing the active site. Zhang et al.[66] have reported the significant role played by Asp 181 situated in the WPD loop in its closure. Kumar et al.[59] have reported the MD study of human PTP1B wherein the flexibility of the WPD loop was observed to be significantly reduced by 10% upon ligand binding. Earlier studies have observed the WPD loop to be rigid in all complexes compared to native $PTP1B_{1\text{-}298a}$ measured using the amino acid flexibility analysis.[40]

We have investigated the flexibility of this WPD loop by measuring the distance between Asp 181 and Cys 215 during the period of simulation. Figure 6a shows a reduction in the distance between the Asp 181 and Cys 215 after 2.5 ns which is observed to decrease further until 10 ns for $PTP1B_{1\text{-}298a}$. Interestingly, in the presence of CGA and CHA, the distance between these two residues did not change much during the entire period of simulation. This clearly shows that $PTP1B_{1\text{-}298a}$ attempts to attain an active state by the closure of Asp 181 over Cys 215 as evidenced by a decrease in the distance of 5.0 Å which was not observed in $PTP1B_{1\text{-}282e}$ (Supporting Information Figure 3). The allosteric inhibitors do not exhibit any decrease in the distance, showing the restriction of PTP1B toward attaining the active state. Analysis of the rmsd profile for the WPD loop showed a stabilized deviation for the $PTP1B_{1\text{-}298a}$, whereas for $PTP1B_{1\text{-}298b}$, $PTP1B_{1\text{-}298c}$, and $PTP1B_{1\text{-}298d}$ the deviation appeared to be inconsistent, clearly revealing the controlled inactivation of the protein (Supporting Information Figure 4). Binding free energies of the protein ligand simulations investigated by calculation of the linear interaction free energy estimate showed the energy values of CGA to be similar to those of compound-2 and maintained consistently throughout the period of simulation (Figure 6b). Analysis of the radius of gyration of $PTP1B_{1\text{-}298a}$, $PTP1B_{1\text{-}298b}$, $PTP1B_{1\text{-}298c}$, and $PTP1B_{1\text{-}298d}$ showed no significant change in $PTP1B_{1\text{-}298c}$ and $PTP1B_{1\text{-}298d}$ confirming that these inhibitors do not cause any aberrant change like unfolding of the protein, though a small difference in their energy values was observed (Supporting Information Figure 5).

The minimum distance between compound-2 and the allosteric site residues Trp 291, Phe 280, Phe 196, and Leu 192 was explored throughout the simulation to confirm the previous observations that the benzofuran core of compound-2 is stacked in a hydrophobic pocket formed by these residues.[62] The average minimum distance between these residues and compound-2 was observed to be 0.3, 0.3, 0.35, and 0.35 nm, respectively, aiding in maintaining the inhibitor to stay at the hydrophobic allosteric pocket (Supporting Information Figure 6). Simulation results with $PTP1B_{1\text{-}298c}$ demonstrates that the minimum distance between Trp 291, Phe 280, Phe 196, and Leu 192 with CGA are 0.25, 0.25, 0.3, and 0.3 nm, respectively (Figure 7), confirming that these hydrophobic interactions

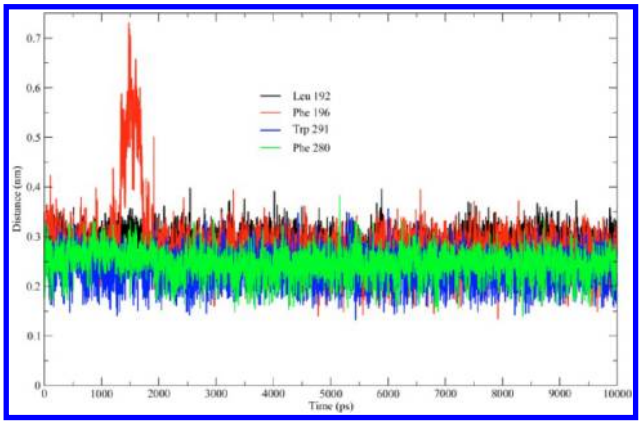

Figure 7. Minimum distance between Trp 291, Phe 280, Phe 196, and Leu 192 with CGA, respectively, profiled in the presence and absence of inhibitors comparatively depicted for the entire 10 ns simulation.

stabilize CGA in the α-3 α-6 α-7 groove due to good binding. Although a deviation in the distance of Phe 280 of around 1.5 ns was observed, it is not largely significant, since the

dx.doi.org/10.1021/ci200581g | J. Chem. Inf. Model. XXXX, XXX, XXX−XXX

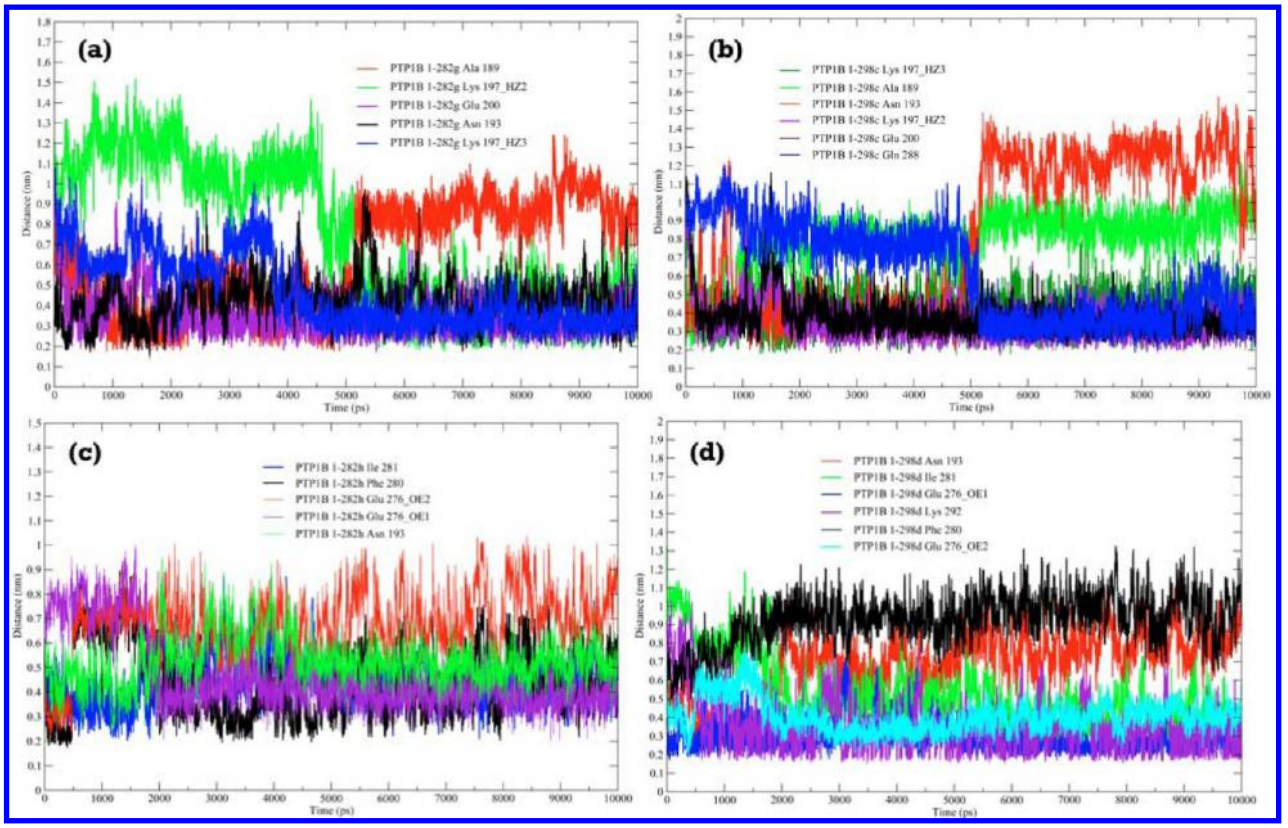

Figure 8. (a) Distance between the hydrogen bonding residues Asn 193, Glu 200, Ala 189, and Lys 197 with CGA in the absence of the α-7 helix ($PTP1B_{1\text{-}282g}$) comparatively depicted for the entire 10 ns simulation. (b) Distance between the hydrogen bonding residues Asn 193, Glu 200, Ala 189, Lys 197 and Gln 288 with CGA in the presence of the α-7 helix ($PTP1B_{1\text{-}298c}$) comparatively depicted for the entire 10 ns simulation. (c) Distance between the hydrogen bonding residues Asn 193, Glu 276, Ile 281, and Phe 280 with CHA in the absence of the α-7 helix ($PTP1B_{1\text{-}282h}$) comparatively depicted for the entire 10 ns simulation. (d) Distance between the hydrogen bonding residues Asn 193, Glu 276, Ile 281, Lys 292, and Phe 280 with CHA in the presence of the α-7 helix ($PTP1B_{1\text{-}298d}$) comparatively depicted for the entire 10 ns simulation.

stabilization of the protein occurs after 2 ns and the observed deviation was very transient. Contrastingly, simulations of $PTP1B_{1\text{-}298d}$ shows that the minimum distance between Trp 291, Phe 280, Phe 196, and Leu 192 with CHA are 0.4, 0.45, 0.25, and 0.25 nm, respectively, clearly showing the inability of CHA to interact with the α-7 helix suggesting it to be a less potent allosteric inhibitor of PTP1B (Supporting Information Figure 7).

To probe the bonding interaction of the ligands with the α-7 helix, simulations were performed in the absence and presence (modeled) of the α-7 helix. The distance profile of the H-bonding residues showed the presence of H-bonds formed with Asn 193 in $PTP1B_{1\text{-}282f}$, which was not observed in $PTP1B_{1\text{-}298b}$.This could be due to an increase in the distance to 7.0 Å between the bonding atoms. A new H-bond formation was observed between Ser 295 of the α-7 helix and the carbonyl oxygen of compound-2 within a range of less than 3.0 Å. The distance of the reference compound-2 with Glu 276 and sulfonamide amino was found to be maintained at < 3.0 Å, showing the stability of the H-Bond in both $PTP1B_{1\text{-}298b}$ and $PTP1B_{1\text{-}282f}$ (Supporting Information Figure 8).

The interaction of CGA with residues of $PTP1B_{1\text{-}282g}$ showed the presence of five hydrogen bonds. Analysis of the distance profile showed the formation of H-bonds by hydroxyl groups of CGA with Lys 197_HZ2, Lys 197_HZ3, Glu 200, and Asn 193 to be maintained below 3.0 Å, whereas an increase to 8 Å was observed for Ala 189 (Figure 8a). From the simulation study performed for $PTP1B_{1\text{-}298c}$, it was observed that, due to an increase in distance of about 9 Å, the interaction of the ligand with Asn 193 and Ala 189 appeared to be lost. The distance with Lys 197 and Glu 200 was found to be below 3 Å, and the formation of a new bond was observed with the hydroxyl group of CGA and Gln 288 during the last 5 ns of simulation (Figure 8b). A similar study with CHA showed interaction with $PTP1B_{1\text{-}282h}$ in the absence of the α-7 helix to be fluctuating. The distance between the ligand and the residues Glu 276_OE1, Phe 280, and Ile 281 were found to be less than 3 Å. Interaction with Asn 193 and Glu 276_OE2 was not observed due to an increase in distance to 5 Å (Figure 8c). During the simulation of CHA with $PTP1B_{1\text{-}298d}$, the interaction with Phe 280 and Asn 193 appeared to be lost. The distance of ligand with Glu 276_OE1 and Glu 276_OE2 was maintained below 3 Å, with the formation of new bond between Lys 292 and hydroxyl group of CGA. The distance with ILE 281 was observed to deviate at (~4 Å) providing a possibility of reduction in interaction with the ligand (Figure 8d).

The outward deviation of the α-7 helix from the protein has been predicted and studied with the known allosteric inhibitor (compound-2).[61] Recently, it has been elucidated through molecular simulations that the α-7 helix plays an important role in the allosteric inhibition of PTP1B. The deviation produced by CGA and CHA on the α-7 helix is demonstrated by an increase in the distance between the residues Glu 200 of the α-3 helix and Met 282 of the α-6 helix (Figure 9a). Further, an increase in distance of 5 Å was observed between Glu 200 of the α-3 helix and Val 287 of the α-7 helix (Figure 9b) which clearly demonstrated the outward movement of the α-7 helix

dx.doi.org/10.1021/ci200581g | J. Chem. Inf. Model. XXXX, XXX, XXX−XXX

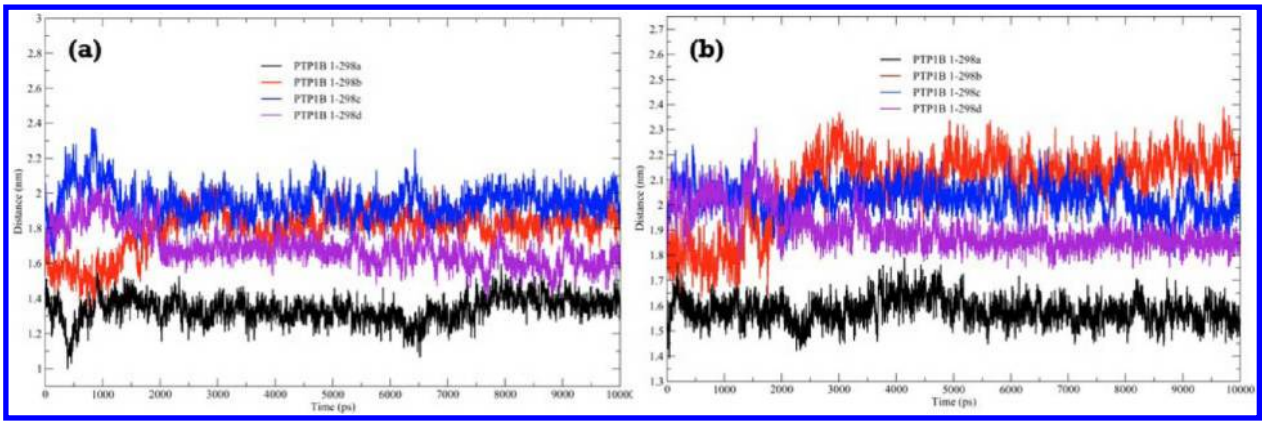

Figure 9. (a) Distance deviation profile between Glu 200 of the α-3 helix and Met 282 of the α-6 helix in the presence and absence of inhibitors depicted for the entire 10 ns simulation. (b) Distance deviation profile between Glu 200 of the α-3 helix and Val 287 of the α-7 helix in the presence and absence of inhibitors depicted for the entire 10 ns simulation.

due to interaction with the ligands. The deviation in distance for CHA was not significant as that of CGA. CGA exhibited minimum deviation of 4 Å throughout the simulation. The distance deviation at the allosteric site was also confirmed by measuring the minimum distance of the C-α of the residues between α-3, α-6, and α-7 helices. These plots clearly show that binding of these inhibitors at the allosteric pocket cause a significant shift in distance of about 4 Å in the case of the α-3 and α-6 helices (Supporting Information Figure 9) and a shift of around 3 Å in the case of the α-3 and α-7 helices (Supporting Information Figure 10).

CONCLUSION

The current study investigated the dynamic interaction of PTP1B with two caffeoyl derivatives, CGA and CHA. Our studies have revealed a noncompetitive inhibition of these compounds compared to vanadium compounds, leading to the hypothesis that they could be allosteric inhibitors of PTP1B which has been evaluated using molecular dynamics studies for a time scale of 10 ns. The study demonstrates that at the allosteric site of PTP1B, there is a significant interaction of CGA and CHA with the α-3, α-6, and α-7 helices. Analyses of the WPD loop flexibility which is in the closed position in the active form of the PTP1B appeared to be restricted upon binding of CGA and CHA due to hindered interaction of the α-3 and α-6 helices with the α-7 helix. The study demonstrates that, at the allosteric site of PTP1B, there is a prominent interaction of CGA with key residues Lys 197, Glu 200, and Gln 288 whereas CHA does not exhibit interaction with these residues due to its binding orientation. CGA was observed to form a better interaction with the α-7 helix providing an insight into the inhibition of the protein. Evidently a reduction in the stability of the catalytic loop was observed in the absence of the α-7 helix. The results clearly show the significant role of the α-7 helix in the inhibition of PTP1B at the allosteric site, via influencing the activation of the WPD loop at the catalytic site. In conclusion, the allosteric site of PTP1B could be playing an important role in its activity and could be a useful target for the screening of antidiabetic compounds.

ASSOCIATED CONTENT

Supporting Information

Additional data regarding the energy and distance deviation profile for the detailed evaluation of protein−ligand simulations as supporting Figures 1−10. This material is available free of charge via the Internet at http://pubs.acs.org.

AUTHOR INFORMATION

Corresponding Author

*E-mail: lakshmibs@annauniv.edu or lakshmibs1@yahoo.com. Tel.: 0091-44-22350772. Fax: 0091-44-22350299.

Notes

The authors declare no competing financial interest.

ACKNOWLEDGMENTS

The authors are grateful to Dr. Satyavani Vemparala, Dr. Raveendra Reddy B, the system administrators of Institute of Mathematical Sciences, Chennai for access to the HPC Aravali3 machine for the molecular simulations, and Dr. Subrata Chattopadhyay (CDAC) and Janaki Chintalapati (CDAC) for providing access to computational resources of the GARUDA Cluster (CDAC). The authors also thank the BTIS-DIC facility of the Centre for Biotechnology, Anna University, Chennai.

REFERENCES

(1) Tony, H. Signaling and Beyond. *Cell* **2000**, *100* (1), 113−127.
(2) Andersen, J. N.; Jansen, P. G.; Echwald, S. M.; Mortensen, O. H.; Fukada, T.; Del Vecchio, R.; Tonks, N. K.; Moller, N. P. H. A genomic perspective on protein tyrosine phosphatases: gene structure, pseudogenes, and genetic disease linkage. *FASEB. J.* **2004**, *18* (1), 8−30.
(3) Tautz, L.; Pellecchia, M.; Mustelin, T. Targeting the PTPome in human disease. *Expert. Opin. Ther. Targets.* **2006**, *10* (1), 157−177.
(4) Van Huijsduijnen, R. H.; Bombrun, A.; Swinnen, D. Selecting protein tyrosine phosphatases as drug targets. *Drug. Discov. Today.* **2002**, *7* (19), 1013−1019.
(5) Fauman, E. B.; Saper, M. A. Structure and function of the protein tyrosine phosphatases. *Trends. Biochem. Sci.* **1996**, *21* (11), 413−417.
(6) Bialy, L.; Waldmann, H. Inhibitors of Protein Tyrosine Phosphatases: Next-Generation Drugs? *Angew. Chem., Int. Ed.* **2005**, *44* (25), 3814−3839.
(7) Kenner, K. A.; Anyanwu, E.; Olefsky, J. M.; Kusari, J. Protein-tyrosine Phosphatase 1B Is a Negative Regulator of Insulin- and Insulin-like Growth Factor-I-stimulated Signaling. *J. Biol. Chem.* **1996**, *271* (33), 19810−19816.
(8) Elchebly, M.; Payette, P.; Michaliszyn, E.; Cromlish, W.; Collins, S.; Loy, A. L.; Normandin, D.; Cheng, A.; Himms Hagen, J.; Chan, C. C.; Ramachandran, C.; Gresser, M. J.; Tremblay, M. L.; Kennedy, B. P. Increased Insulin Sensitivity and Obesity Resistance in Mice Lacking

the Protein Tyrosine Phosphatase-1B Gene. *Science* **1999**, *283* (5407), 1544−1548.
(9) Klaman, L. D.; Boss, O.; Peroni, O. D.; Kim, J. K.; Martino, J. L.; Zabolotny, J. M.; Moghal, N.; Lubkin, M.; Kim, Y.-B.; Sharpe, A. H.; Stricker-Krongrad, A.; Shulman, G. I.; Neel, B. G.; Kahn, B. B. Increased Energy Expenditure, Decreased Adiposity, and Tissue-Specific Insulin Sensitivity in Protein-Tyrosine Phosphatase 1B-Deficient Mice. *Mol. Cell. Biol.* **2000**, *20* (15), 5479−5489.
(10) Johnson, T. O.; Ermolieff, J.; Jirousek, M. R. Protein tyrosine phosphatase 1B inhibitors for diabetes. *Nat. Rev. Drug. Discov.* **2002**, *1* (9), 696−709.
(11) Byon, J. C. H.; Kusari, A. B.; Kusari, J. Protein-tyrosine phosphatase-1B acts as a negative regulator of insulin signal transduction. *Mol. Cell. Biochem.* **1998**, *182* (1), 101−108.
(12) Ramachandran, C.; Kennedy, B. P. Protein Tyrosine Phosphatase 1B: A Novel Target for Type 2 Diabetes and Obesity. *Curr. Top. Med. Chem.* **2003**, *3* (7), 749−757.
(13) Koren, S.; Fantus, I. G. Inhibition of the protein tyrosine phosphatase PTP1B: potential therapy for obesity, insulin resistance and type-2 diabetes mellitus. *Best. Pract. Res. Clin. Endocrinol. Metab.* **2007**, *21* (4), 621−640.
(14) Puius, Y. A.; Zhao, Y.; Sullivan, M.; Lawrence, D. S.; Almo, S. C.; Zhang, Z.-Y. Identification of a second aryl phosphate-binding site in protein-tyrosine phosphatase 1B: A paradigm for inhibitor design. *Proc. Natl. Acad. Sci. USA* **1997**, *94* (25), 13420−13425.
(15) Barford, D.; Flint, A.; Tonks, N. Crystal structure of human protein tyrosine phosphatase 1B. *Science* **1994**, *263* (5152), 1397−1404.
(16) Montalibet, J.; Skorey, K.; McKay, D.; Scapin, G.; Asante-Appiah, E.; Kennedy, B. P. Residues Distant from the Active Site Influence Protein-tyrosine Phosphatase 1B Inhibitor Binding. *J. Biol. Chem.* **2006**, *281* (8), 5258−5266.
(17) Jia, Z.; Barford, D.; Flint, A.; Tonks, N. Structural basis for phosphotyrosine peptide recognition by protein tyrosine phosphatase 1B. *Science* **1995**, *268* (5218), 1754−1758.
(18) Pedersen, A. K.; Peters, G. H.; Moller, K. B.; Iversen, L. F.; Kastrup, J. S. Water-molecule network and active-site flexibility of apo protein tyrosine phosphatase 1B. *Acta. Crystallogr. D. Biol. Crystallogr.* **2004**, *60* (9), 1527−1534.
(19) Kolmodin, K.; Åqvist, J. The catalytic mechanism of protein tyrosine phosphatases revisited. *FEBS. Lett.* **2001**, *498* (2−3), 208−213.
(20) Doina, P. Novel protein tyrosine phosphatase 1B inhibitors: interaction requirements for improved intracellular efficacy in type 2 diabetes mellitus and obesity control. *Biochem. Biophys. Res. Commun.* **2011**, *410* (3), 377−381.
(21) Iversen, L. F.; Andersen, H. S.; Branner, S.; Mortensen, S. B.; Peters, G. H.; Norris, K.; Olsen, O. H.; Jeppesen, C. B.; Lundt, B. F.; Ripka, W.; Møller, K. B.; Møller, N. P. H. Structure-based Design of a Low Molecular Weight, Nonphosphorus, Nonpeptide, and Highly Selective Inhibitor of Protein-tyrosine Phosphatase 1B. *J. Biol. Chem.* **2000**, *275* (14), 10300−10307.
(22) Shen, K.; Keng, Y.-F.; Wu, L.; Guo, X.-L.; Lawrence, D. S.; Zhang, Z.-Y. Acquisition of a Specific and Potent PTP1B Inhibitor from a Novel Combinatorial Library and Screening Procedure. *J. Biol. Chem.* **2001**, *276* (50), 47311−47319.
(23) Liljebris, C.; Martinsson, J.; Tedenborg, L.; Williams, M.; Barker, E.; Duffy, J. E. S.; Nygren, A.; James, S. Synthesis and biological activity of a novel class of pyridazine analogues as non-competitive reversible inhibitors of protein tyrosine phosphatase 1B (PTP1B). *Bioorg. Med. Chem.* **2002**, *10* (10), 3197−3212.
(24) Sun, J.-P.; Fedorov, A. A.; Lee, S.-Y.; Guo, X.-L.; Shen, K.; Lawrence, D. S.; Almo, S. C.; Zhang, Z.-Y. Crystal Structure of PTP1B Complexed with a Potent and Selective Bidentate Inhibitor. *J. Biol. Chem.* **2003**, *278* (14), 12406−12414.
(25) Xie, L.; Lee, S. Y.; Andersen, J. N.; Waters, S.; Shen, K.; Guo, X.-L.; Moller, N. P. H.; Olefsky, J. M.; Lawrence, D. S.; Zhang, Z. Y. Cellular Effects of Small Molecule PTP1B Inhibitors on Insulin Signaling. *Biochemistry* **2003**, *42* (44), 12792−12804.
(26) Cheon, H. G.; Kim, S. M.; Yang, S. D.; Ha, J. D.; Choi, J. K. Discovery of a novel protein tyrosine phosphatase-1B inhibitor, KR61639: potential development as an antihyperglycemic agent. *Eur. J. Pharmacol.* **2004**, *485* (1−3), 333−339.
(27) Black, E.; Breed, J.; Breeze, A. L.; Embrey, K.; Garcia, R.; Gero, T. W.; Godfrey, L.; Kenny, P. W.; Morley, A. D.; Minshull, C. A.; Pannifer, A. D.; Read, J.; Rees, A.; Russell, D. J.; Toader, D.; Tucker, J. Structure-based design of protein tyrosine phosphatase-1B inhibitors. *Bioorg. Med. Chem. Lett.* **2005**, *15* (10), 2503−2507.
(28) Combs, A. P.; Yue, E. W.; Bower, M.; Ala, P. J.; Wayland, B.; Douty, B.; Takvorian, A.; Polam, P.; Wasserman, Z.; Zhu, W.; Crawley, M. L.; Pruitt, J.; Sparks, R.; Glass, B.; Modi, D.; McLaughlin, E.; Bostrom, L.; Li, M.; Galya, L.; Blom, K.; Hillman, M.; Gonneville, L.; Reid, B. G.; Wei, M.; Becker-Pasha, M.; Klabe, R.; Huber, R.; Li, Y.; Hollis, G.; Burn, T. C.; Wynn, R.; Liu, P.; Metcalf, B. Structure-Based Design and Discovery of Protein Tyrosine Phosphatase Inhibitors Incorporating Novel Isothiazolidinone Heterocyclic Phosphotyrosine Mimetics. *J. Med. Chem.* **2005**, *48* (21), 6544−6548.
(29) Klopfenstein, S. R.; Evdokimov, A. G.; Colson, A.-O.; Fairweather, N. T.; Neuman, J. J.; Maier, M. B.; Gray, J. L.; Gerwe, G. S.; Stake, G. E.; Howard, B. W.; Farmer, J. A.; Pokross, M. E.; Downs, T. R.; Kasibhatla, B.; Peters, K. G. 1,2,3,4-Tetrahydroisoquinolinyl sulfamic acids as phosphatase PTP1B inhibitors. *Bioorg. Med. Chem. Lett.* **2006**, *16* (6), 1574−1578.
(30) Moretto, A. F.; Kirincich, S. J.; Xu, W. X.; Smith, M. J.; Wan, Z. K.; Wilson, D. P.; Follows, B. C.; Binnun, E.; Joseph-McCarthy, D.; Foreman, K.; Erbe, D. V.; Zhang, Y. L.; Tam, S. K.; Tam, S. Y.; Lee, J. Bicyclic and tricyclic thiophenes as protein tyrosine phosphatase 1B inhibitors. *Bioorg. Med. Chem. Lett.* **2006**, *14* (7), 2162−2177.
(31) Wan, Z. K.; Lee, J.; Xu, W.; Erbe, D. V.; Joseph-McCarthy, D.; Follows, B. C.; Zhang, Y. L. Monocyclic thiophenes as protein tyrosine phosphatase 1B inhibitors: Capturing interactions with Asp48. *Bioorg. Med. Chem. Lett.* **2006**, *16* (18), 4941−4945.
(32) Yue, E. W.; Wayland, B.; Douty, B.; Crawley, M. L.; McLaughlin, E.; Takvorian, A.; Wasserman, Z.; Bower, M. J.; Wei, M.; Li, Y.; Ala, P. J.; Gonneville, L.; Wynn, R.; Burn, T. C.; Liu, P. C. C.; Combs, A. P. Isothiazolidinone heterocycles as inhibitors of protein tyrosine phosphatases: Synthesis and structure−activity relationships of a peptide scaffold. *Bioorg. Med. Chem. Lett.* **2006**, *14* (17), 5833−5849.
(33) Combs, A. P.; Zhu, W.; Crawley, M. L.; Glass, B.; Polam, P.; Sparks, R. B.; Modi, D.; Takvorian, A.; McLaughlin, E.; Yue, E. W.; Wasserman, Z.; Bower, M.; Wei, M.; Rupar, M.; Ala, P. J.; Reid, B. M.; Ellis, D.; Gonneville, L.; Emm, T.; Taylor, N.; Yeleswaram, S.; Li, Y.; Wynn, R.; Burn, T. C.; Hollis, G.; Liu, P. C. C.; Metcalf, B. Potent Benzimidazole Sulfonamide Protein Tyrosine Phosphatase 1B Inhibitors Containing the Heterocyclic (S)-Isothiazolidinone Phosphotyrosine Mimetic. *J. Med. Chem.* **2006**, *49* (13), 3774−3789.
(34) Jacqueline, M.; Brian, P. K. Therapeutic strategies for targeting PTP1B in diabetes. *Drug. Discov. Today. Ther. Strateg.* **2005**, *2* (2), 129−135.
(35) Vintonyak, V. V.; Antonchick, A. P.; Rauh, D.; Waldmann, H. The therapeutic potential of phosphatase inhibitors. *Curr. Opin. Chem. Biol.* **2009**, *13* (3), 272−283.
(36) Erbe, D. V.; Klaman, L. D.; Wilson, D. P.; Wan, Z. K.; Kirincich, S. J.; Will, S.; Xu, X.; Kung, L.; Wang, S.; Tam, S.; Lee, J.; Tobin, J. F. Prodrug delivery of novel PTP1B inhibitors to enhance insulin signalling. *Diabetes. Obes. Metab.* **2009**, *11* (6), 579−588.
(37) Stuible, M.; Doody, K.; Tremblay, M. PTP1B and TC-PTP: regulators of transformation and tumorigenesis. *Cancer. Metastasis. Rev.* **2008**, *27* (2), 215−230.
(38) Wiesmann, C.; Barr, K. J.; Kung, J.; Zhu, J.; Erlanson, D. A.; Shen, W.; Fahr, B. J.; Zhong, M.; Taylor, L.; Randal, M.; McDowell, R. S.; Hansen, S. K. Allosteric inhibition of protein tyrosine phosphatase 1B. *Nat. Struct. Mol. Biol.* **2004**, *11* (8), 730−737.
(39) Kamerlin, S. C. L.; Rucker, R.; Boresch, S. A targeted molecular dynamics study of WPD loop movement in PTP1B. *Biochem. Biophys. Res. Commun.* **2006**, *345* (3), 1161−1166.

(40) Kamerlin, S. C. L.; Rucker, R.; Boresch, S. A molecular dynamics study of WPD-loop flexibility in PTP1B. *Biochem. Biophys. Res. Commun.* **2007**, *356* (4), 1011−1016.
(41) Olmez, E. O.; Alakent, B. Alpha7 Helix Plays an Important Role in the Conformational Stability of PTP1B. *J. Biomol. Struct. Dyn.* **2011**, *28* (5), 675−843.
(42) Muthusamy, V. S.; Anand, S.; Sangeetha, K. N.; Sujatha, S.; Arun, B.; Lakshmi, B. S. Tannins present in Cichorium intybus enhance glucose uptake and inhibit adipogenesis in 3T3-L1 adipocytes through PTP1B inhibition. *Chem. Biol. Interact.* **2008**, *174* (1), 69−78.
(43) Muthusamy, V. S.; Saravanababu, C.; Ramanathan, M.; Bharathi Raja, R.; Sudhagar, S.; Anand, S.; Lakshmi, B. S. Inhibition of protein tyrosine phosphatase 1B and regulation of insulin signalling markers by caffeoyl derivatives of chicory (Cichorium intybus) salad leaves. *Br. J. Nutr.* **2010**, *104* (06), 813−823.
(44) Doman, T. N.; McGovern, S. L.; Witherbee, B. J.; Kasten, T. P.; Kurumbail, R.; Stallings, W. C.; Connolly, D. T.; Shoichet, B. K. Molecular Docking and High-Throughput Screening for Novel Inhibitors of Protein Tyrosine Phosphatase-1B. *J. Med. Chem.* **2002**, *45* (11), 2213−2221.
(45) Huang, P.; Ramphal, J.; Wei, J.; Liang, C.; Jallal, B.; McMahon, G.; Tang, C. Structure-Based design and discovery of novel inhibitors of protein tyrosine phosphatases. *Bioorg. Med. Chem.* **2003**, *11* (8), 1835−1849.
(46) Zhou, M.; Ji, M. Molecular docking and 3D-QSAR on 2-(oxalylamino) benzoic acid and its analogues as protein tyrosine phosphatase 1B inhibitors. *Bioorg. Med. Chem.* **2005**, *15* (24), 5521−5525.
(47) Cummings, M. D.; DesJarlais, R. L.; Gibbs, A. C.; Mohan, V.; Jaeger, E. P. Comparison of Automated Docking Programs as Virtual Screening Tools. *J. Med. Chem.* **2005**, *48* (4), 962−976.
(48) Goel, A.; Dixit, M.; Saeed, U.; Kumar, A.; Siddiqi, M. I.; Tamrakar, A. K.; Srivastava, A. K. Synthesis, Molecular Docking and PTP1B Inhibitory Activity of Functionalized 4,5-Dihydronaphthofurans and Dibenzofurans. *Med. Chem.* **2008**, *4* (1), 18−24.
(49) Dias, D. M.; Teixeira, J. M. C.; Kuprov, I.; New, E. J.; Parker, D.; Geraldes, C. F. G. C. Enantioselective binding of a lanthanide(iii) complex to human serum albumin studied by 1H STD NMR techniques. *Org. Biomol. Chem.* **2011**, *9* (14), 5047−5050.
(50) Ellingson, S. R.; Baudry, J. High-throughput virtual molecular docking: Hadoop implementation of AutoDock4 on a private cloud. In *Proceedings of the second international workshop on Emerging computational methods for the life sciences (ECMLS '11)*; ACM: San Jose, California, USA, 2011; pp 33−38; http://dl.acm.org/citation.cfm?id=1996028 (accessed Nov 13, 2011).
(51) Lill, M.; Danielson, M. Computer-aided drug design platform using PyMOL. *J. Comput. Aided. Mol. Des.* **2011**, *25* (1), 13−19.
(52) Rousaki, A.; Miyata, Y.; Jinwal, U. K.; Dickey, C. A.; Gestwicki, J. E.; Zuiderweg, E. R. P. Allosteric Drugs: The Interaction of Antitumor Compound MKT-077 with Human Hsp70 Chaperones. *J. Mol. Biol.* **2011**, *411* (3), 614−632.
(53) Schuttelkopf, A. W.; Van Aalten, D. M. F. PRODRG: a tool for high-throughput crystallography of protein-ligand complexes. *Acta. Crystallogr. D. Biol. Crystallogr.* **2004**, *60* (8), 1355−1363.
(54) Pettersen, E. F.; Goddard, T. D.; Huang, C. C.; Couch, G. S.; Greenblatt, D. M.; Meng, E. C.; Ferrin, T. E. UCSF Chimera—A visualization system for exploratory research and analysis. *J. Comput. Chem.* **2004**, *25* (13), 1605−1612.
(55) Sanner, M. F. Python: a programming language for software integration and development. *J. Mol. Graphics. Mod.* **1999**, *17* (1), 57−61.
(56) Goodsell, D. S.; Morris, G. M.; Olson, A. J. Automated docking of flexible ligands: Applications of autodock. *J. Mol. Recognit.* **1996**, *9* (1), 1−5.
(57) Morris, G. M.; Goodsell, D. S.; Halliday, R. S.; Huey, R.; Hart, W. E.; Belew, R. K.; Olson, A. J. Automated docking using a Lamarckian genetic algorithm and an empirical binding free energy function. *J. Comput. Chem.* **1998**, *19* (14), 1639−1662.
(58) Eswar, N.; Webb, B.; Marti-Renom, M. A.; Madhusudhan, M. S.; Eramian, D.; Shen, M.-y.; Pieper, U.; Sali, A. Comparative Protein Structure Modeling Using Modeller. In *Current Protocols in Bioinformatics*; John Wiley & Sons, Inc.: New York, 2002.
(59) Kumar, R.; Shinde, R. N.; Ajay, D.; Sobhia, M. E. Probing Interaction Requirements in PTP1B Inhibitors: A Comparative Molecular Dynamics Study. *J. Chem. Inf. Model.* **2010**, *50* (6), 1147−1158.
(60) Peters, G. H.; Frimurer, T. M.; Andersen, J. N.; Olsen, O. H. Molecular Dynamics Simulations of Protein-Tyrosine Phosphatase 1B. I. Ligand-Induced Changes in the Protein Motions. *Biophys. J.* **1999**, *77* (1), 505−515.
(61) Bharatham, K.; Bharatham, N.; Kwon, Y.; Lee, K. Molecular dynamics simulation study of PTP1B with allosteric inhibitor and its application in receptor based pharmacophore modeling. *J. Comput. Aided. Mol. Des.* **2008**, *22* (12), 925−933.
(62) Wang, J.-F.; Gong, K.; Wei, D.-Q.; Li, Y.-X. Structural flexibility and interactions of PTP1B's S-loop. *Interdiscip. Sci.* **2009**, *1* (3), 214−219.
(63) Van Der Spoel, D.; Lindahl, E.; Hess, B.; Groenhof, G.; Mark, A. E.; Berendsen, H. J. C. GROMACS: Fast, flexible, and free. *J. Comput. Chem.* **2005**, *26* (16), 1701−1718.
(64) Hess, B.; Kutzner, C.; Van der Spoel, D.; Lindahl, E. GROMACS 4: Algorithms for Highly Efficient, Load-Balanced, and Scalable Molecular Simulation. *J. Chem. Theory. Comput.* **2008**, *4* (3), 435−447.
(65) Paul, T. *Xmgrace (Grace): free WYSIWYG 2D graph plotting tool, for Unix-like operating systems.* http://plasma-gate.weizmann.ac.il/Grace/(accessed June 2, 2012).
(66) Zhang, Z. Y.; Wang, Y.; Wu, L.; Fauman, E. B.; Stuckey, J. A.; Schubert, H. L.; Saper, M. A.; Dixon, J. E. The Cys(X)5Arg Catalytic Motif in Phosphoester Hydrolysis. *Biochemistry* **1994**, *33* (51), 15266−15270.